Fault Modeling, Estimation, and Fault-Tolerant Steering Logic Design for Single-Gimbal Control Moment Gyro

Qiang Shen, Chengfei Yue, Xiang Yu, and Cher Hiang Goh

***Abstract*— This brief addresses the single-gimbal control moment gyro (SGCMG) fault modeling, estimation, and tolerant-control steering logic design problem, aiming at enhancing the reliability and safety of spacecraft attitude control systems. The SGCMG is modeled as a two-loop system, including a wheel speed control loop and a gimbal rate control loop. Each loop contains an electrical motor (EM) and its corresponding variable speed drive (VSD), which may suffer from faults. By analyzing and modeling potential faults of the EM-VSD system, the SGCMG fault model is further developed. Then, a local adaptive fault estimator is proposed to reconstruct the total time-varying fault effects of each SGCMG. It is proven that the gimbal angle estimation error and fault estimation error converge to small compact sets containing zero. Moreover, leveraging estimated fault effects, a fault-tolerant steering logic is further developed to allocate the commanded attitude control torque properly such that the gimbal rate constraints are satisfied, and fault effects are compensated. To verify the proposed fault estimator and fault-tolerant steering logic, numerical simulations are carried out on an SGCMG-actuated spacecraft.**

***Index Terms*— Control moment gyro (CMG), fault modeling, fault-tolerant control, steering law.**

I. Introduction

IN PRACTICAL space missions, redundant momentum exchange devices, such as reaction wheels (RWs) and control moment gyro (CMG), are equipped in spacecraft to enhance the reliability, maneuverability, and survivability. However, if a fault occurs in momentum exchange devices, their output torques acting on the spacecraft may be different from commands required by the attitude controller, which may lead to performance deterioration or even instability of the whole system. For instance, the Mars Odyssey (launched in 2001) came into protective standby mode in 2014 due to the failure of an RW. How to avoid space mission failure and the economic losses caused by faults in momentum exchange devices have attracted a great deal of interest in the field of spacecraft control.

To enhance the system reliability and compensate for the adverse effect induced by actuator faults in spacecraft missions, a proper fault model representing most of the potential faults for momentum exchange devices is crucial. In [1], the mechanism of RW fault is analyzed, but a mathematical model is not given explicitly. In [2]–[4], a mathematical model consisting of an effectiveness gain matrix and a bias vector is proposed to represent four different kinds of RW faults. In contrast to RW, since CMG has a complex structure and working principle, it is not straightforward to develop a proper fault model representing most of CMG fault modes. Although general motor faults in CMGs of the small satellite are analyzed in [5], the CMG fault model is not developed. In [6], a fault model is proposed to describe the loss of effectiveness and bias in the gimbal rate control loop. However, the mechanism of CMG fault is not clearly analyzed and the general CMG fault model is not established in [6].

After developing a proper actuator fault model, fault reconstruction and fault-tolerant control need to be addressed. Many results have been proposed for tackling RW faults. Using a radial basis function neural network to estimate RW fault, an adaptive control allocation method is proposed to redistribute control effects to fault-free RWs in [7]. In [8], a local adaptive observer and a finite-time fault-tolerant controller are designed to estimate and accommodate RW fault, respectively. Based on the reconstructed fault from an indirect fault estimator, a fault-tolerant backstepping controller is synthesized to compensate fault effects despite actuator saturation constraints in [9]. In contract to the RW-based fault-tolerant control design, there are very few fault-tolerant control results on CMG. In [10], the skew angle of a pyramid CMG configuration is tuned through a genetic algorithm to handle CMG failures. In [6], the sliding mode control approach is adapted to change the CMG gimbal rate directly to avoid singularities and deal with CMG faults without fault estimation. Since the worst case fault is considered for designing the sliding mode controller, this method is conservative from the perspective of control performance.

In this brief, a fault-tolerant control system consisting of fault modeling, estimation, and fault-tolerant steering logic is proposed for single-gimbal CMG (SGCMG)-actuated spacecraft. The SGCMG is considered to be an integration of two electric motor and variable speed drive (EM-VSD) systems. By analyzing potential faults and their corresponding effects, a multiplicative effectiveness factor and an additive offset are introduced to represent faults in an EM-VSD system. Then, an SGCMG fault model in a cascade multiplication form of

Manuscript received July 27, 2019; accepted February 1, 2020. Manuscript received in final form February 2, 2020. This work was supported by the National Science Foundation of China under Grant 61833013 and Grant 61973012. Recommended by Associate Editor A. Serrani. *(Corresponding author: Chengfei Yue.)*

Qiang Shen is with the School of Aeronautics and Astronautics, Shanghai Jiao Tong University, Shanghai 200240, China (e-mail: qiang.shen@sjtu.edu.cn).

Chengfei Yue is with the Institute of Space Science and Applied Technology, Harbin Institute of Technology, Shenzhen 518055, China (e-mail: yuechengfei@hit.edu.cn).

Xiang Yu is with the School of Automation Science and Electrical Engineering and the Beijing Advanced Innovation Center for Big Data-Based Precision Medicine, Beihang University, Beijing 100191, China (e-mail: xiangyu1110@gmail.com).

Cher Hiang Goh is with the Department of Electrical and Computer Engineering, National University of Singapore, Singapore 119077 (e-mail: elegch@nus.edu.sg).

Color versions of one or more of the figures in this article are available online at http://ieeexplore.ieee.org.

Digital Object Identifier 10.1109/TCST.2020.2971959

This article has been accepted for inclusion in a future issue of this journal. Content is final as presented, with the exception of pagination.

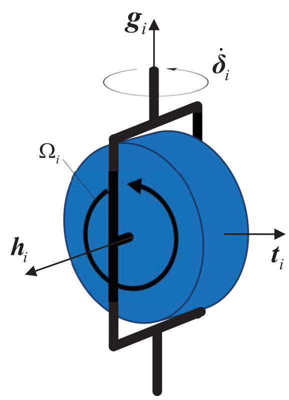

Fig. 1. Schematic of an SGCMG.

two EM-VSD systems is established. Inspired by the results in [8] and [11], we design local adaptive estimators to reconstruct total fault effects in gimbal rate control loop for each SGCMG. In contrast to existing fault estimators, such as [3] and [9], which only obtain the resultant effect caused by all actuator faults, the developed local fault estimator aims to obtain a more accurate fault estimation by distinguishing and estimating the fault effect on each individual actuator. Moreover, leveraging the obtained fault information, we proposed a Karush–Kuhn–Tucker (KKT) condition-based fault-tolerant SGCMG steering logic, which not only compensates the fault influences but also avoids/escapes the SGCMG singularity by selecting suitable weighting matrices. To the best of our knowledge, this is the first attempt to accommodate SGCMG fault in the actuator level by constructing a fault-tolerant steering logic instead of in attitude controller design. When compared with the general singular robust (GSR) steering logic in [12] and [13], the proposed approach has advantages of fault accommodation and guaranteed gimbal rate constraints while dealing with singularities. Finally, the effectiveness of the proposed SGCMG fault estimator and fault-tolerant steering logic is demonstrated through numerical simulation.

The remaining part of this brief is organized as follows. Section II introduces the mathematical models of the EM-VSD system and SGCMG. Section III develops a local fault estimator. The fault-tolerant steering logic is proposed in Section IV. In Section V, numerical simulation on a rigid spacecraft using four SGCMGs is carried out to verify the proposed fault estimator and fault-tolerant steering logic. Finally, this brief ends with the conclusion in Section VI.

II. SGCMG Fault Model

Due to the advantages of simple structure and high torque amplification capability, the SGCMG is frequently used as an actuator in agile spacecraft to ensure fast attitude maneuver and high pointing precision. As shown in Fig. 1, the SGCMG is a constant-speed rotor mounted on a gimbal frame such that the direction of angular momentum keeps changing, but its magnitude is a constant. The SGCMG can be considered as an integration of a gimbal rotation control system and a wheel speed control system from its mechanical structure. Since either the gimbal control loop or wheel speed control loop can be modeled as an EM-VSD system, the SGCMG is regarded as a cascade combination of two independent EM-VSD systems [14], which describe dynamics of the rotor control loop and the gimbal frame control loop, respectively. The potential faults of an SGCMG may occur in the mechanical and/or electrical system of the EMs and the sensors and actuators of the VSDs in both the rotor control loop and the wheel speed control loop. In this section, we develop an SGCMG fault model that generalizes the existing fault models used in [2]–[6].

A. Fault Model of EM-VSD System

The detailed faults in an EM-VSD system are given in [15]–[18]. Specifically, for the EM, potential faults are categorized into [17]: bearing faults, stator or mature faults, broken rotor bar and end ring faults of induction machines, and eccentricity-related faults. With regard to VSD, faults are classified into mechanical and electrical faults, actuator faults (actuator in VSD), and sensor faults.

In general, mechanical faults (e.g., faulty bearings, brush wear, shaft misalignment, eccentric rotor, and so on) and electrical faults (e.g., broken rotor bars, windings short-circuit, and so on) in an EM-VSD system are induced by mechanical wearing, harsh working environment, aging, and severe voltage stresses. These faults belong to multiplicative faults that can be represented by the change of output effectiveness. In addition, actuator fault in VSD would cause insufficient voltages or currents to drive an EM. The sensors in VSD may also suffer from faults such that the physical phenomenon cannot be characterized properly. These faults are considered as additive faults [18], [19], which have effects similar to measurement bias or external disturbances.

According to a recent work in [14], fault models of the two EM-VSD systems in an SGCMG are given by

$$\begin{cases} \Omega = \eta_\Omega \Omega_c + \Omega_a, & \text{Rotor speed control loop} \\ \dot{\delta} = \eta_\delta \dot{\delta}_c + \dot{\delta}_a, & \text{Gimbal rate control loop} \end{cases} \tag{1}$$

where Ω and Ω_c are rotating speed of flywheel and its command input, $\dot{\delta}$ and $\dot{\delta}_c$ are gimbal rate output and its command from SGCMG steering law, η_Ω and η_δ denote effectiveness gains satisfying $0 \leq \eta_\Omega \leq 1$ and $0 \leq \eta_\delta \leq 1$, and Ω_a and $\dot{\delta}_a$ are bounded offsets.

B. SGCMG Fault Model

As shown in Fig. 1, the torque generated by an SGCMG is proportional to the plane spanned by the angular momentum vector and gimbal angular rate vector and is computed as:

$$\tau = -h_0 \dot{\delta} \hat{t} \tag{2}$$

where h_0 denotes the constant angular momentum of the spinning rotor, and $\hat{t}$ denotes a unit vector in the direction of output torque. The negative sign in (2) implies the output torque lies in the opposite direction of $\hat{t}$.

The potential faults in an SGCMG may exist in the rotor speed control loop and/or gimbal angle control loop. For the rotor control system, the angular momentum is the product of its inertia J_Ω and the rotor angular velocity Ω, i.e., $h_0 = J_\Omega \Omega$. With consideration of the possible faults in rotor speed control loop, which is modeled in (1), the rotor momentum subject to faults is described as:

$$h_0 = J_\Omega(\eta_\Omega \Omega_c + \Omega_a). \tag{3}$$

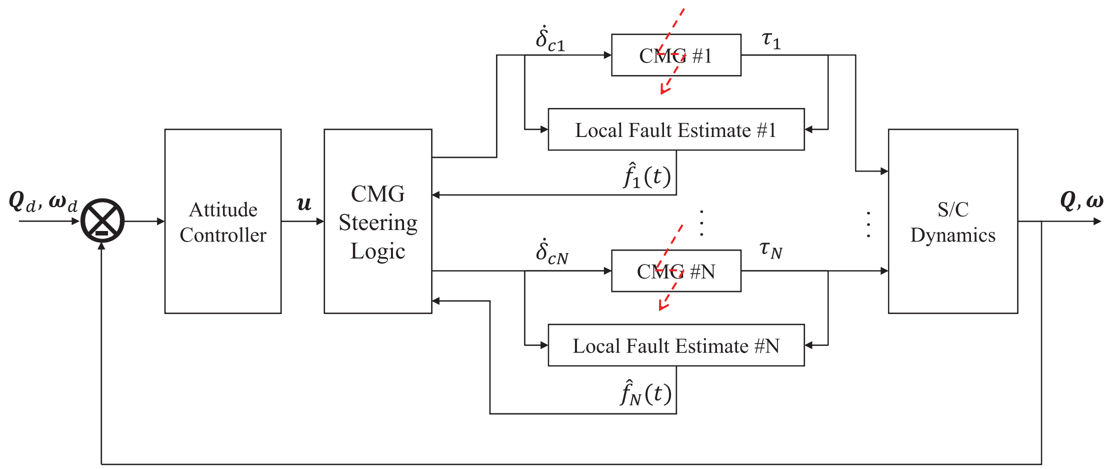

Fig. 2. Overall attitude control system with local fault estimators.

Moreover, in the light of the fault model of gimbal rate control loop in (1), the output torque generated by an SGCMG in the presence of faults is given by

$$\tau = -J_{\Omega}(\eta_{\Omega}\Omega_c + \Omega_a)(\eta_{\delta}\dot{\delta}_c + \dot{\delta}_a)\hat{t}. \tag{4}$$

To this end, we develop the SGCMG fault model considering potential faults in both the rotor speed control loop and the gimbal control loop. From (4), different combinations of η_{Ω}, Ω_a, η_{δ}, and $\dot{\delta}_a$ represent different SGCMG working conditions, including fault modes and nominal situation. Noting that the constraints on the maximum output of the rotor speed and the gimbal rate are not considered in (4) since they are physical limitations of SGCMG rather than faults.

III. Fault Estimation for SGCMG

In Section II, we consider SGCMG as a cascade combination of two EM-VSD systems and then develop fault models for the rotor speed control loop and gimbal rate control loop, respectively. If a fault occurs in the rotor, the undesired rotor speed can be recognized easily through rotational speed measurement as the rotor is supposed to rotate at a constant speed. Therefore, the rotor fault is not considered in this section, and we only propose a fault estimation scheme for the SGCMG gimbal control loop. In practical missions, multiple SGCMGs are employed to generate the commanded torques from an attitude controller. Here, we assume that N SGCMGs are equipped in the spacecraft, and each of N SGCMGs may encounter faults. To obtain the fault information in each SGCMG, we develop a local fault estimator for each SGCMG. The overall attitude control system with local fault estimation is demonstrated in Fig. 2.

Recalling (1), the gimbal fault model can be written as

$$\dot{\delta} = \dot{\delta}_c + f \tag{5}$$

where $f = (\eta_{\delta} - 1)\dot{\delta}_c + \dot{\delta}_a$ represents the total fault effect lumping the loss of effectiveness fault and additive offset. The commanded gimbal rate $\dot{\delta}_c$ is computed from the SGCMG steering logic, which is assumed to be known in fault estimator design and will be given in Section IV.

Assumption 1: The total fault effect f in each SGCMG is differentiable, and its time derivative is bounded such that $|\dot{f}| \leq \overline{f}$, where $\overline{f}$ is a positive constant.

In the proposed fault estimation approach, we estimate the total fault effect f in each SGCMG rather than each individual gains η_{δ} and $\dot{\delta}_a$. If we proceed to estimate individual actuator fault, the fault estimation approach may become complicated and time consuming, especially when several kinds of fault occur concurrently in an SGCMG.

To estimate the total fault effect f in an SGCMG, we first define an auxiliary variable as [9], [20]

$$\xi = f - k\delta \tag{6}$$

where k is a positive constant. Next, the local adaptive estimator for fault estimation is proposed as follows:

$$\dot{\hat{\delta}} = \dot{\delta}_c + \alpha(\delta - \hat{\delta}) + \hat{f} \tag{7}$$

$$\dot{\hat{\xi}} = -k\dot{\delta}_c - k\hat{\xi} - k^2\hat{\delta} \tag{8}$$

where α is a positive design parameter chosen by the designer. Define estimation errors $\tilde{\delta} = \delta - \hat{\delta}$ and $\tilde{\xi} = \xi - \hat{\xi}$. Based on (6), fault estimation error is expressed as $\tilde{f} = \tilde{\xi} + k\tilde{\delta}$. Thus, estimation error dynamics can be derived as

$$\dot{\tilde{\delta}} = -(\alpha - k)\tilde{\delta} + \tilde{\xi} \tag{9}$$

$$\dot{\tilde{\xi}} = -k\tilde{\xi} - k^2\tilde{\delta} + \dot{f}. \tag{10}$$

Theorem 1: Considering the gimbal fault model in (5) with loss of effectiveness fault and additive bias fault satisfying Assumption 1, applying the proposed local adaptive estimator consisting of a state estiamtion (7) and an auxiliary variable estimation (8) with the parameter constraints defined in (13) and (14), the gimbal angle estimate error and fault estimate error ultimately converge to small compact sets containing zero.

Proof: Consider the following Lyapunov candidate:

$$V = \frac{1}{2}\tilde{\delta}^2 + \frac{1}{2}\tilde{\xi}^2. \tag{11}$$

Taking time derivative of V along with (9) and (10) yields

$$\begin{aligned}\dot{V} &= -(\alpha - k)\tilde{\delta}^2 - k\tilde{\xi}^2 - (k^2 - 1)\tilde{\delta}\tilde{\xi} + \dot{f}\tilde{\xi} \\ &\leq -(\alpha - k)\tilde{\delta}^2 - \left(k - \frac{\epsilon}{2}\right)\tilde{\xi}^2 - (k^2 - 1)\tilde{\delta}\tilde{\xi} + \frac{1}{2\epsilon}\overline{f}^2\end{aligned}$$

where the inequality $\dot{f}\tilde{\xi} \le \epsilon/2\tilde{\xi}^2 + 1/2\epsilon\overline{f}^2$ and Assumption 1 are used. The foregoing inequality can be further written as

$$\dot{V} \le -\begin{bmatrix}\tilde{\delta} & \tilde{\xi}\end{bmatrix} \boldsymbol{P} \begin{bmatrix}\tilde{\delta} & \tilde{\xi}\end{bmatrix}^{\mathrm{T}} + \varrho, \tag{12}$$

where $\boldsymbol{P} = \begin{bmatrix}\alpha - k & \frac{1}{2}(k^2-1) \\ * & k - \frac{\epsilon}{2}\end{bmatrix}$ and $\varrho = 1/2\epsilon\overline{f}^2$. If parameters α, k, and ϵ are selected to satisfy

$$k - \alpha < 0 \tag{13}$$

$$k^4 + 2k^2 - (2\alpha + \epsilon)k + \alpha\epsilon + 1 < 0 \tag{14}$$

then the matrix $\boldsymbol{P}$ is positive-definite. Consequently, we have $\dot{V} < -\kappa \mathrm{V} + \rho$ with $\kappa = 2\lambda_{\min}(P)$. Moreover, it is clear that $\dot{V} < 0$ when

$$|\tilde{\delta}(t)| > \sqrt{\frac{\varrho}{\lambda_{\min}(P)}} \ \texttt{or}\ |\tilde{\xi}(t)| > \sqrt{\frac{\varrho}{\lambda_{\min}(P)}}. \tag{15}$$

Therefore, $\tilde{\delta}$ and $\tilde{\xi}$ exponentially converge to compact sets $\mathbb{S}_{\tilde{\delta}}$ and $\mathbb{S}_{\tilde{\xi}}$ with rates greater than $e^{-\kappa t}$, where

$$\mathbb{S}_{\tilde{\delta}} = \left\{\tilde{\delta} \middle| |\tilde{\delta}| \le \sqrt{\frac{\varrho}{\lambda_{\min}(P)}}\right\} \tag{16}$$

$$\mathbb{S}_{\tilde{\xi}} = \left\{\tilde{\xi} \middle| |\tilde{\xi}| \le \sqrt{\frac{\varrho}{\lambda_{\min}(P)}}\right\}. \tag{17}$$

In addition, since $\tilde{f} = \tilde{\xi} + \mathrm{k}\tilde{\delta}$, the fault estimation error converges to the set $\mathbb{S}_{\tilde{f}}$ defined as

$$\mathbb{S}_{\tilde{f}} = \left\{\tilde{f} \middle| |\tilde{f}| \le (k+1)\sqrt{\frac{\varrho}{\lambda_{\min}(P)}}\right\}. \tag{18}$$

This completes the proof. ■

IV. Fault-Tolerant Steering Logic

In this section, we proposed a fault-tolerant SGCMG steering logic to allocate the torque calculated from attitude controller to each SGCMG while compensating effects caused by gimbal faults.

A. Spacecraft Attitude Error Dynamics

To address the attitude tracking problem, the desired attitude and the desired angular velocity of the spacecraft in the desired reference frame $\mathcal{B}_d$ with respect to inertial frame $\mathcal{I}$ are denoted by unit quaternion $\boldsymbol{Q}_d = \begin{bmatrix}\boldsymbol{q}_d^{\mathrm{T}} \ q_{d0}\end{bmatrix}^{\mathrm{T}} \in \mathbb{R}^3 \times \mathbb{R}$ and $\boldsymbol{\omega}_d \in \mathbb{R}^3$, respectively. The attitude tracking error $\boldsymbol{Q}_e = \begin{bmatrix}\boldsymbol{q}_e^{\mathrm{T}} \ q_{e0}\end{bmatrix}^{\mathrm{T}} \in \mathbb{R}^3 \times \mathbb{R}$ is defined as the relative orientation between attitude $\boldsymbol{Q} = \begin{bmatrix}\boldsymbol{q}^{\mathrm{T}} \ q_0\end{bmatrix}^{\mathrm{T}} \in \mathbb{R}^3 \times \mathbb{R}$ and target attitude $\boldsymbol{Q}_d$ and is computed as $\boldsymbol{Q}_e = \boldsymbol{Q}_d^{-1} \otimes \boldsymbol{Q}$, where $\boldsymbol{Q}_d^{-1}$ is the inverse or conjugate of the desired quaternion determined by $\boldsymbol{Q}_d^{-1} = \begin{bmatrix}-\boldsymbol{q}_d^{\mathrm{T}} \ q_{d0}\end{bmatrix}^{\mathrm{T}}$, and "$\otimes$" denotes the quaternion multiplication operator of two unit quaternion. The angular velocity error $\boldsymbol{\omega}_e \in \mathbb{R}^3$ describing the discrepancy between the inertia angular velocity $\boldsymbol{\omega} \in \mathbb{R}^3$ and the desired one $\boldsymbol{\omega}_d$ is given by $\boldsymbol{\omega}_e = \boldsymbol{\omega} - \boldsymbol{C}\boldsymbol{\omega}_d$, where $\boldsymbol{C}$ is the rotation matrix that is defined as $\boldsymbol{C} = (q_{e0}^2 - \boldsymbol{q}_e^{\mathrm{T}}\boldsymbol{q}_e)\boldsymbol{I}_3 + 2\boldsymbol{q}_e\boldsymbol{q}_e^{\mathrm{T}} - 2q_{e0}\boldsymbol{q}_e^{\times}$ with $\boldsymbol{I}_3 \in \mathbb{R}^{3\times 3}$ denoting a 3×3 identity matrix and the notation $\boldsymbol{x}^{\times} \in \mathbb{R}^{3\times 3}$ representing the skew-symmetric cross-product matrix for a vector $\boldsymbol{x} = \begin{bmatrix}x_1 \ x_2 \ x_3\end{bmatrix}^{\mathrm{T}} \in \mathbb{R}^3$. Then, the attitude tracking error system can be expressed by the following equations [21]:

$$\begin{cases}\boldsymbol{J}\dot{\boldsymbol{\omega}}_e = -(\boldsymbol{\omega}_e + \boldsymbol{C}\boldsymbol{\omega}_d)^{\times}\boldsymbol{J}(\boldsymbol{\omega}_e + \boldsymbol{C}\boldsymbol{\omega}_d) \\ \quad + \boldsymbol{J}(\boldsymbol{\omega}_e^{\times}\boldsymbol{C}\boldsymbol{\omega}_d - \boldsymbol{C}\dot{\boldsymbol{\omega}}_d) + \boldsymbol{\tau}_a + \boldsymbol{d} \\ \dot{\boldsymbol{q}}_e = \dfrac{1}{2}(\boldsymbol{q}_e^{\times} + q_{e0}\boldsymbol{I}_3)\boldsymbol{\omega}_e \\ \dot{q}_{e0} = -\dfrac{1}{2}\boldsymbol{q}_e^{\mathrm{T}}\boldsymbol{\omega}_e.\end{cases} \tag{19}$$

where $\boldsymbol{J} \in \mathbb{R}^{3\times 3}$ denotes the positive definite inertia matrix of the spacecraft, $\boldsymbol{\tau}_a \in \mathbb{R}^3$ denotes the internal control torque produced by N identical SGCMGs, and $\boldsymbol{d} \in \mathbb{R}^3$ is the bounded external disturbance.

B. SGCMG Steering Logic Design

The steering law is to be designed such that N SGCMGs realize the commanded control torque $\boldsymbol{u} \in \mathbb{R}^3$ from the attitude controller. Many attitude tracking controllers have been proposed to achieve a stable attitude tracking with satisfactory performance in the literature, for example, proportional-derivative (PD) controller [21], adaptive controller [22], [23], inverse optimal controller [24], and so on. Since the major focus of this brief is not on attitude controller design, it is assumed that there exists an attitude controller that provides stable attitude tracking in the following steering logic design.

For a given control torque command $\boldsymbol{u}$, the internal control torque generated by N SGCMG should satisfy

$$\boldsymbol{\tau}_a = \boldsymbol{\tau} - \boldsymbol{\omega}^{\times}\boldsymbol{h} = \boldsymbol{u} \tag{20}$$

where $\boldsymbol{\tau} = -h_0\overline{\boldsymbol{A}}\dot{\boldsymbol{\delta}} \in \mathbb{R}^3$ is the total torque generated by N SGCMGs, h_0 is magnitude of nominal angular momentum, $\overline{\boldsymbol{A}} \in \mathbb{R}^{3\times N}$ is the Jacobian matrix of derivative of $\boldsymbol{h}$, $\boldsymbol{h} \in \mathbb{R}^3$ is angular momentum produced by SGCMG cluster, and $\dot{\boldsymbol{\delta}} = [\dot{\delta}_1, \ldots, \dot{\delta}_N]^{\mathrm{T}} \in \mathbb{R}^N$ is the actual gimbal rate.

Considering SGCMG gimbal fault modeled in (5), the actual gimbal rate output $\dot{\boldsymbol{\delta}}$ and the gimbal rate command $\dot{\boldsymbol{\delta}}_c = [\dot{\delta}_{c,1}, \ldots, \dot{\delta}_{c,N}]^{\mathrm{T}} \in \mathbb{R}^N$ have the following relationship:

$$\dot{\boldsymbol{\delta}} = \dot{\boldsymbol{\delta}}_c + \boldsymbol{f}. \tag{21}$$

To compensate the total SGCMG fault effects, the estimated fault information $\hat{\boldsymbol{f}} = [\hat{f}_1, \ldots, \hat{f}_N]^{\mathrm{T}}$ from Section III is used to replace the actual fault $\boldsymbol{f} = [f_1, \ldots, f_N]^{\mathrm{T}}$ in steering logic design. Then, substituting (21) into (20), the commanded gimbal rate $\dot{\boldsymbol{\delta}}_c$ of N SGCMGs in the presence of faults is chosen such that

$$-h_0\overline{\boldsymbol{A}}(\dot{\boldsymbol{\delta}}_c + \hat{\boldsymbol{f}}) - \boldsymbol{\omega}^{\times}\boldsymbol{h} = \boldsymbol{u}. \tag{22}$$

Inspired by the work in [25], to distribute the command torque to each individual SGCMG in the presence of faults, a fault-tolerant steering logic is computed through solving the following optimization problem:

$$\min_{\dot{\boldsymbol{\delta}}_c} \ J(\dot{\boldsymbol{\delta}}_c) = \frac{1}{2}\|h_0\overline{\boldsymbol{A}}(\dot{\boldsymbol{\delta}}_c + \hat{\boldsymbol{f}}) + \boldsymbol{\omega}^{\times}\boldsymbol{h} + \boldsymbol{u}\|_{\boldsymbol{W}}^2 + \frac{1}{2}\|\dot{\boldsymbol{\delta}}_c\|_{\boldsymbol{Q}}^2 \tag{23}$$

$$\text{s.t. } \dot{\boldsymbol{\delta}}_c - \boldsymbol{r}_{\min} \ge 0,\ \boldsymbol{r}_{\max} - \dot{\boldsymbol{\delta}}_c \ge 0 \tag{24}$$

where $\|h_0\overline{\boldsymbol{A}}(\dot{\boldsymbol{\delta}}_c + \hat{\boldsymbol{f}}) + \boldsymbol{\omega}^{\times}\boldsymbol{h} + \boldsymbol{u}\|_{\boldsymbol{W}}^2$ stands for $(h_0\overline{\boldsymbol{A}}(\dot{\boldsymbol{\delta}}_c + \hat{\boldsymbol{f}}) + \boldsymbol{\omega}^{\times}\boldsymbol{h} + \boldsymbol{u})^{\mathrm{T}}\boldsymbol{W}(h_0\overline{\boldsymbol{A}}(\dot{\boldsymbol{\delta}}_c + \hat{\boldsymbol{f}}) + \boldsymbol{\omega}^{\times}\boldsymbol{h} + \boldsymbol{u})$, $\|\dot{\boldsymbol{\delta}}_c\|_{\boldsymbol{Q}}^2$ stands for $\dot{\boldsymbol{\delta}}_c^{\mathrm{T}}\boldsymbol{Q}\dot{\boldsymbol{\delta}}_c$, $\boldsymbol{Q} \in \mathbb{R}^{N\times N}$ and $\boldsymbol{W} \in \mathbb{R}^{3\times 3}$ are two symmetric positive-definite matrices, and $\boldsymbol{r}_{\min}$ and $\boldsymbol{r}_{\max}$ are SGCMGs' lower and upper bounds on the gimbal rate.

To reduce the notational burden, we define $\boldsymbol{G} = h_0\overline{\boldsymbol{A}}$ and $\boldsymbol{v} = -\boldsymbol{u} - h_0\overline{\boldsymbol{A}}\hat{\boldsymbol{f}} - \boldsymbol{\omega}^{\times}\boldsymbol{h}$. Then, the proposed fault-tolerant steering logic design problem can be written as

$$\min_{\dot{\boldsymbol{\delta}}_c} \ J(\dot{\boldsymbol{\delta}}_c) = \frac{1}{2}\|\boldsymbol{G}\dot{\boldsymbol{\delta}}_c - \boldsymbol{v}\|_{\boldsymbol{W}}^2 + \frac{1}{2}\|\dot{\boldsymbol{\delta}}_c\|_{\boldsymbol{Q}}^2 \tag{25}$$

$$\text{s.t. } \dot{\boldsymbol{\delta}}_c - \boldsymbol{r}_{\min} \geq 0, \ \boldsymbol{r}_{\max} - \dot{\boldsymbol{\delta}}_c \geq 0. \tag{26}$$

To solve the minimization problem, a Lagrangian function is defined as

$$L(\dot{\boldsymbol{\delta}}_c, \boldsymbol{\lambda}_1, \boldsymbol{\lambda}_2) = J(\dot{\boldsymbol{\delta}}_c) - \boldsymbol{\lambda}_1^{\mathrm{T}}(\dot{\boldsymbol{\delta}}_c - \boldsymbol{r}_{\min}) - \boldsymbol{\lambda}_2^{\mathrm{T}}(\boldsymbol{r}_{\max} - \dot{\boldsymbol{\delta}}_c) \tag{27}$$

where the Lagrangian multipliers $\boldsymbol{\lambda}_1 \in \mathbb{R}^N$ and $\boldsymbol{\lambda}_2 \in \mathbb{R}^N$ are nonnegative vectors. Based on the KKT condition, the optimal solution $\dot{\boldsymbol{\delta}}_c^*$ with $\boldsymbol{\lambda}_1^*$ and $\boldsymbol{\lambda}_2^*$ satisfies [26]

$$\boldsymbol{G}^{\mathrm{T}}\boldsymbol{W}(\boldsymbol{G}\dot{\boldsymbol{\delta}}_c^* - \boldsymbol{v}) + \boldsymbol{Q}\dot{\boldsymbol{\delta}}_c^* - \boldsymbol{\lambda}_1^* + \boldsymbol{\lambda}_2^* = 0, \tag{28}$$

$$\lambda_{1,i}^*\left(\dot{\delta}_{c,i}^* - r_{\min,i}\right) = 0, \ \lambda_{2,i}^*\left(r_{\max,i} - \dot{\delta}_{c,i}^*\right) = 0, \tag{29}$$

$$\dot{\boldsymbol{\delta}}_c^* - \boldsymbol{r}_{\min} \geq 0, \ \boldsymbol{r}_{\max} - \dot{\boldsymbol{\delta}}_c^* \geq 0, \tag{30}$$

$$\boldsymbol{\lambda}_1^* \geq 0, \ \boldsymbol{\lambda}_2^* \geq 0 \tag{31}$$

where $\lambda_{1,i}^*$, $\lambda_{2,i}^*$, $r_{\min,i}$, $r_{\max,i}$, and $\dot{\delta}_{c,i}^*$ are the ith row of $\boldsymbol{\lambda}_1^*$, $\boldsymbol{\lambda}_2^*$, $\boldsymbol{r}_{\min}$, $\boldsymbol{r}_{\max}$, and $\dot{\boldsymbol{\delta}}_c^*$ for $i = 1, \ldots, N$, respectively.

Generally speaking, the KKT conditions are only the necessary conditions for finding the global minima of nonlinear programming problems. If both the objective function and the constraints are convex, the KKT conditions are also sufficient to obtain the global optimality. Otherwise, extra examinations are required to exclude the local minima and the maximum. Based on the constraints from KKT condition, we find that the optimal gimbal rate $\dot{\boldsymbol{\delta}}_{c,i}^*$ are classified by the values of Lagrangian multipliers $\boldsymbol{\lambda}_1^*$ and $\boldsymbol{\lambda}_2^*$. When the Lagrangian multipliers $\boldsymbol{\lambda}_1^* = 0$ and/or $\boldsymbol{\lambda}_2^* = 0$, the optimal gimbal rate $\dot{\boldsymbol{\delta}}_c^*$ is free from the complementary slackness and computed within its boundaries by solving the algebraic equations (28). When the Lagrangian multipliers $\boldsymbol{\lambda}_1^* \neq 0$ and/or $\boldsymbol{\lambda}_2^* \neq 0$, the optimal gimbal rate $\dot{\boldsymbol{\delta}}_c^*$ is constrained to be the value of $\boldsymbol{r}_{\min}$ or $\boldsymbol{r}_{\max}$ from the complementary slackness (29). As a consequence, several local minima and the boundary values are obtained from the earlier two classified steps. Finally, further comparisons among these local minima and the boundary values should be included to find the global minimum, which produces the smallest value of cost function.

In summary, based on the KKT conditions, the algorithm for solving the fault-tolerant steering logic design problem formulated (25) and (26) is implemented as follows.

Inputs:

1) Calculate $\boldsymbol{G}$ and $\boldsymbol{v}$ based on gimbal angle measurement, high-level controller, fault estimation scheme, and SGCMG specification.
2) Choose the weighting parameters $\boldsymbol{W}$ and $\boldsymbol{Q}$.

Steps:

1) Let $\lambda_{j,i}$ be the elements of vectors $\boldsymbol{\lambda}_1$ and $\boldsymbol{\lambda}_2$ for $j \in \{1, 2\}$ and $i \in \{1, \ldots, N\}$.
2) Let k be the number of nonzero elements. Since $\lambda_{1,i}$ and $\lambda_{2,i}$ cannot be nonzero at the same time, we have $k \in \{0, \ldots, N\}$.
3) Set $k = 0$.
4) Find all $\binom{N}{k}2^k$ combinations of (j, i) for k nonzero $\lambda_{j,i}$.
5) Corresponding to each combination of (j, i) in Step 4, set k of $\lambda_{j,i}$ to be nonzero and $2N - k$ remaining $\lambda_{j,i}$ to be zero, and consequently obtain $\dot{\boldsymbol{\delta}}_{c,i}^*$ (for instance, for $k = 2$, if $\lambda_{1,1} \neq 0$ and $\lambda_{2,2} \neq 0$, then $\dot{\boldsymbol{\delta}}_{c,1}^* = r_{\min,1}$ and $\dot{\boldsymbol{\delta}}_{c,2}^* = r_{\max,2}$). The other $\dot{\boldsymbol{\delta}}_{c,i}^*$ in each combination, when there are k nonzero elements in $\lambda_{j,i}$, can be computed by solving the remaining algebraic equations in (28).
6) Assign $k := k + 1$. If $k \leq N$, then go to Step 4. Otherwise, compute the values of cost function for all the $\dot{\boldsymbol{\delta}}_c^*$ (there are $\sum_{k=0}^{N}\binom{N}{k}2^k = 3^N$ different combinations in total), and find the global optimal $\dot{\boldsymbol{\delta}}_c^*$ by comparison.

Remark 1: In Step 5 of the earlier algorithm, we need to solve an algebraic equation in (28). Define matrices $\boldsymbol{\Pi} = \mathrm{G}^T\mathrm{W}\mathrm{G} + \boldsymbol{Q}$ and $\boldsymbol{\Theta} = \mathrm{G}^T\mathrm{W}\mathrm{v} + \boldsymbol{\lambda}_1^* - \boldsymbol{\lambda}_2^*$. Since the weighting matrices $\boldsymbol{W}$ and $\boldsymbol{Q}$ are positive-definite, $\boldsymbol{\Pi}$ is always nonsingular, and hence, the solution of (28) can be given as $\dot{\boldsymbol{\delta}}_c^* = \boldsymbol{\Pi}^{-1}\boldsymbol{\Theta}$. Moreover, to deal with the SGCMG singularity, we need to select the weighting matrices $\boldsymbol{W}$ and $\boldsymbol{Q}$ properly such that the proposed steering logic can avoid or escape all kinds of singularities, while the existing control allocation method in [25] cannot solve this problem directly. Inspired by the singularity escape/avoidance steering logic in [13], we select $\boldsymbol{W} = \boldsymbol{W}_{\text{inv}}^{-1} > 0$ and $\boldsymbol{Q} = \boldsymbol{Q}_{\text{inv}}^{-1} > 0$, where

$$\boldsymbol{W}_{\text{inv}} = \gamma\begin{bmatrix} 1 & \zeta_3 & \zeta_2 \\ \zeta_3 & 1 & \zeta_1 \\ \zeta_2 & \zeta_1 & 1 \end{bmatrix}, \quad \boldsymbol{Q}_{\text{inv}} = \begin{bmatrix} \beta_1 & \gamma & \gamma & \gamma \\ \gamma & \beta_2 & \gamma & \gamma \\ \gamma & \gamma & \beta_3 & \gamma \\ \gamma & \gamma & \gamma & \beta_4 \end{bmatrix}$$

$$\zeta_i = \zeta_0 \sin(\varpi t + \phi_i), \quad \gamma = \gamma_0 \exp[-\mu \det(\overline{\boldsymbol{A}}\,\overline{\boldsymbol{A}}^{\mathrm{T}})]$$

for the case $N = 4$, i.e., there are four SGCMGs in attitude control systems. The design parameters ζ_0, ϖ, ϕ_i $(i = 1, 2, 3)$ and β_j $(j = 1, \ldots, N)$ need to be appropriately chosen such that $\mathrm{G}^T\mathrm{W}\mathrm{v} \neq 0$ for any nonzero $\boldsymbol{v}$ [13].

V. Numerical Simulation

To verify the effectiveness of the proposed fault identification method and fault-tolerant steering logic, numerical simulations for attitude control of an SGCMG-actuated rigid spacecraft subject to gimbal faults are performed.

A. Simulation Specifications

In the simulation, the spacecraft has an inertia $\boldsymbol{J} = \left[10\ 1.2\ 0.5;\ 1.2\ 19\ 1.5;\ 0.5\ 1.5\ 25\right]$ kg·m^2 [28]. The environmental disturbance model is $\boldsymbol{d}(t) = \left[-0.005\sin(t)\ 0.005\sin(t)\ -0.005\sin(t)\right]^{\mathrm{T}}$ N·m [29]. The initial attitude of the spacecraft is assumed to be $\boldsymbol{Q}(0) = \left[-0.5\ 0.3\ -0.4\ 0.7071\right]^{\mathrm{T}}$, while the initial angular velocity is $\boldsymbol{\omega}(0) = \left[0\ 0\ 0\right]^{\mathrm{T}}$ deg/s. Throughout the simulation, we consider a rest-to-rest three-axis attitude maneuver, in

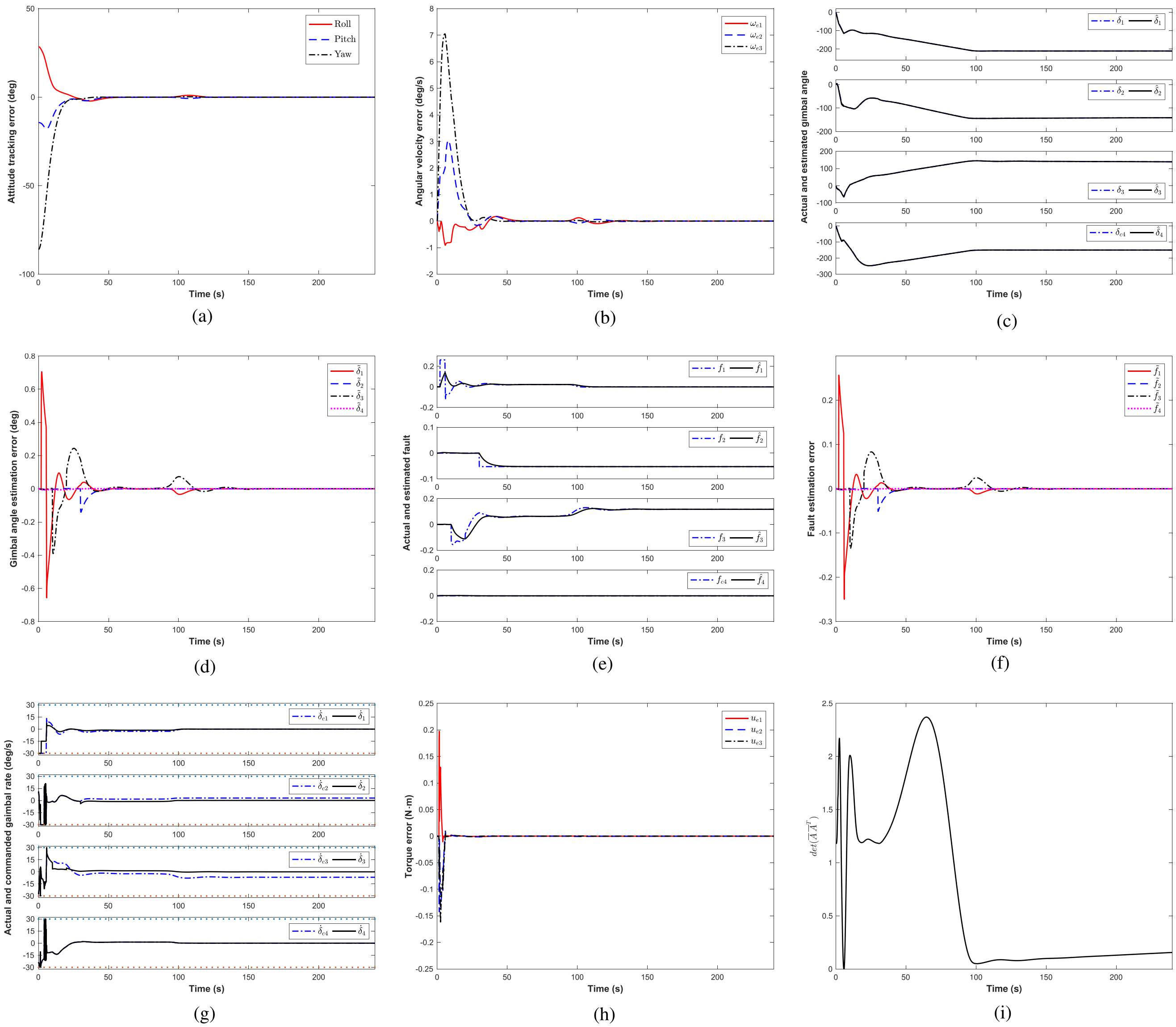

Fig. 3. Attitude control performance under proposed control scheme using local adaptive fault estimator and KKT-based fault-tolerant steering logic. (a) Attitude tracking error. (b) Angular velocity tracking error. (c) Actual and estimated gimbal angle. (d) Gimbal angle estimation error. (e) Actual and estimated fault. (f) Fault estimation error. (g) Actual and commanded gimbal rate. (h) Torque error. (i) Singularity measure.

which the target attitude is $\boldsymbol{Q}_d(0) = \left[0\ 0.8660\ 0\ 0.5\right]^{\mathrm{T}}$. Four identical SGCMGs in a regular pyramid configuration with skew angle $\beta = 54.74$ deg are used as actuators. The magnitude of nominal angular momentum of each SGCMG is 1 N·m·s, and gimbal rate constraints are $r_{\min,i} = -30$ deg/s and $r_{\max,i} = 30$ deg/s ($i = 1, \ldots, 4$). As the CMG systems are generally spun up from a zero-momentum configuration [30], initial gimbal angles are set as $\boldsymbol{\delta}(0) = \left[0\ 0\ 0\ 0\right]^{\mathrm{T}}$ deg.

According to the gimbal fault model in (1), the fault in SGCMG can be described by two parameters $\eta_{\delta,i}$ and $\dot{\delta}_{a,i}$ for SGCMG #i ($i = 1, \ldots, 4$). In the simulation, we assume that the SGCMG #1 can only supply 50% of the commanded gimbal rate after $t = 2$ s, the SGCMG #2 experiences additive offset fault at $t = 30$ s with the size of $\dot{\delta}_{a,2} = -3$ deg/s, the SGCMG #3 is assumed to suffer from partial loss of effectiveness fault at $t = 10$ s with $\eta_{\delta,3} = 0.3$ and additive offset fault at $t = 20$ s with $\dot{\delta}_{a,2} = 2$ deg/s, and the SGCMG #4 is fault-free throughout the simulation. If the proposed fault-tolerant attitude control system can handle these severe SGCMG faults, it can also deal with the less-severe SGCMG faults or fault-free situation.

To achieve three-axis attitude control, the quaternion feedback PD controller is applied, which is designed as [21]

$$\boldsymbol{u} = -k_p \boldsymbol{J}\boldsymbol{q}_e - k_d \boldsymbol{J}\boldsymbol{\omega}_e + \boldsymbol{\omega}^{\times}\boldsymbol{J}\boldsymbol{\omega} - \boldsymbol{J}\left(\boldsymbol{\omega}_e^{\times}\boldsymbol{C}\boldsymbol{\omega}_d - \boldsymbol{C}\dot{\boldsymbol{\omega}}_d\right) \quad (32)$$

where control gains $k_p = 0.1422$ and $k_d = 0.5333$ are selected such that the closed-loop attitude dynamics is critical damping and the settling time of the attitude is around 30 s in fault-free situation. In addition, the magnitude of the PD controller is limited to be less than 1 N·m. The parameters in the weighting matrices of the proposed fault-tolerant steering logic are selected as: $\zeta_0 = 0.01$, $\varpi = 10$, $\phi_1 = 0$, $\phi_2 = \pi/2$, $\phi_3 = \pi$, $\beta_1 = 20$, $\beta_1 = 30$, $\beta_1 = 50$, and $\beta_1 = 10$. To have a fast fault estimation, the fault estimator gains are selected as $\alpha = 20$ and $k = 0.2$, which satisfy the corresponding estimator constraints defined in (13) and (14) when $\epsilon = 0.1$.

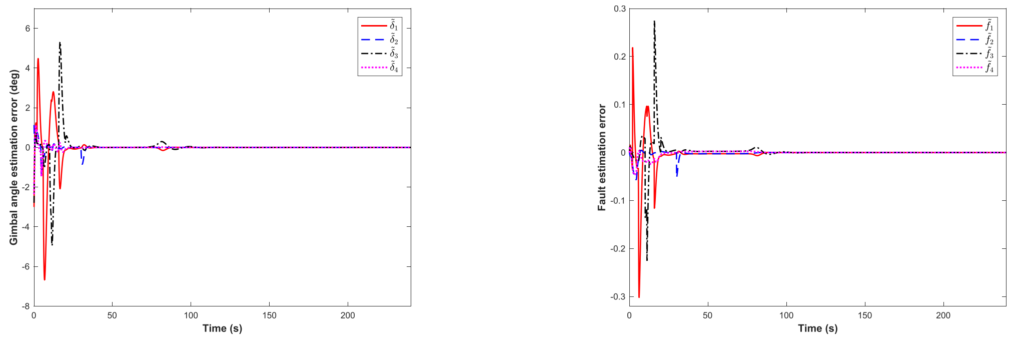

(a) (b)

Fig. 4. Attitude control performance under control scheme using local iterative learning fault estimator [27] and KKT-based fault-tolerant steering logic. (a) Gimbal angle estimation error. (b) Fault estimation error.

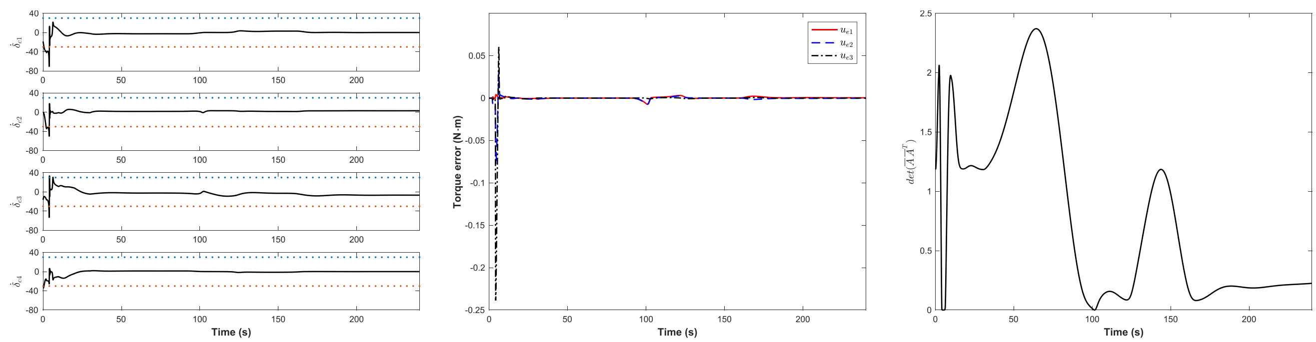

(a) (b) (c)

Fig. 5. Attitude control performance under control scheme using local adaptive fault estimator and fault-tolerant GSR steering logic [12]. (a) Commanded gimbal rate. (b) Torque error. (c) Singularity measure.

B. Result Analysis

The simulation results of the proposed control scheme using local adaptive fault estimator and KKT-based fault-tolerant steering logic are shown in Fig. 3. It is observed from Fig. 3(a) and (b) that attitude and angular velocity tracking errors converge to a neighborhood of zero despite SGCMG gimbal faults. Fig. 3(c)–(f) shows the responses of the gimbal angle and fault estimation errors using the proposed local adaptive fault estimator, from which it is clear that the time-varying gimbal angle and SGCMG fault are estimated accurately. Although the actual gimbal rate response in Fig. 3(g) deviates from the gimbal rate command due to SGCMG faults, the torque error reaches a small bounded region of $\pm 2 \times 10^{-4}$ N·m in 38.1 s, as observed in Fig. 3(h). In addition, the magnitude of the commanded gimbal rate is less than 30 deg/s throughout the simulation, which illustrates that the proposed steering logic ensures gimbal rate constraints effectively. The singularity measure $\det(\overline{\mathbf{A}\mathbf{A}}^{\mathrm{T}})$ is shown in Fig. 3(i), from which we see that a saturated singularity is encountered at 5.6 s due to the loss of effectiveness fault of SGCMG #1. However, this saturated singularity is quickly passed through. Moreover, the steering logic also avoids another internal singularity observed around 90 s in Fig. 3(i) so that the influence of the internal singularity on state tracking and fault estimation could be tolerable.

To demonstrate the advantages of the proposed fault-tolerant system, we also compare the proposed adaptive estimator with the iterative learning observer developed in [27]. Both two estimators are implemented locally for each SGCMG to estimate time-varying gimbal faults. To make the comparison fair, the same PD controller and KKT-based steering logic are used in attitude control. Although both two estimators converge the fault estimation error, the maximum transient error of gimbal angle estimation and fault estimation (6.68 deg and 0.31) under the iterative learning estimator shown in Fig. 4(a) and (b) are larger than that (0.71 deg and 0.26) under the proposed estimator shown in Fig. 3(d) and (f). In addition, the proposed estimator also has a smoother error response than the one using the method in [27]. Finally, we compare the proposed KKT-based steering logic with the GSR steering logic in [12]. It is clear from Fig. 5 that the GSR steering logic cannot ensure the gimbal rate constraint and takes a longer time to escape the saturated singularity. Since the internal singularity is not avoided by the GSR steering logic, an obvious torque error around 90 s is observed in Fig. 5(b). Nevertheless, the proposed KKT-based steering logic does not have these disadvantages.

VI. CONCLUSION

In this brief, we designed a fault-tolerant control scheme for spacecraft attitude control systems to handle SGCMG faults. We consider SGCMG as a combination of two independent EM-VSD systems, which describe the rotor speed control loop and gimbal rate control loop separately. Then, the SGCMG fault model is obtained by multiplying two EM-VSD fault models together. Based on this SGCMG fault model, the total fault effect instead of each individual fault is estimated by a local adaptive estimator, which can exponentially converge fault estimation error with satisfactory accuracy.

Moreover, incorporating the estimated fault information, a fault-tolerant steering logic is further proposed to accommodate SGCMG gimbal fault and singularity. Finally, the effectiveness of the proposed SGCMG fault estimation approach and fault-tolerant steering logic is demonstrated by numerical simulations. As one of the future works, an experimental study of the proposed fault-tolerant system is also important from an application point of view.

References

[1] S. Murugesan and P. Goel, "Fault-tolerant spacecraft attitude control system," *Sadhana*, vol. 11, nos. 1–2, pp. 233–261, 1987.

[2] J. Jin, S. Ko, and C.-K. Ryoo, "Fault tolerant control for satellites with four reaction wheels," *Control Eng. Pract.*, vol. 16, no. 10, pp. 1250–1258, Oct. 2008.

[3] B. Xiao, Q. Hu, W. Singhose, and X. Huo, "Reaction wheel fault compensation and disturbance rejection for spacecraft attitude tracking," *J. Guid., Control, Dyn.*, vol. 36, no. 6, pp. 1456–1575, Nov./Dec. 2013.

[4] Q. Shen, D. Wang, S. Zhu, and K. Poh, "Finite-time fault-tolerant attitude stabilization for spacecraft with actuator saturation," *IEEE Trans. Aerosp. Electron. Syst.*, vol. 51, no. 3, pp. 2390–2405, Jul. 2015.

[5] Y.-C. Choi, J.-H. Son, and H.-S. Ahn, "Fault detection and isolation for a small CMG-based satellite: A fuzzy Q-learning approach," *Aerosp. Sci. Technol.*, vol. 47, pp. 340–355, Dec. 2015.

[6] F. Zhang, L. Jin, and S. Xu, "Fault Tolerant Attitude Control for spacecraft with SGCMGs under actuator partial failure and actuator saturation," *Acta Astronautica*, vol. 132, pp. 303–311, Mar. 2017.

[7] P. Baldi, M. Blanke, P. Castaldi, N. Mimmo, and S. Simani, "Adaptive ftc based on control allocation and fault accommodation for satellite reaction wheels," in *Proc. 3rd Conf. Control Fault-Tolerant Syst. (SysTol)*, Sep. 2016, pp. 672–677.

[8] S. Zhu, D. Wang, Q. Shen, and E. K. Poh, "Satellite attitude stabilization control with actuator faults," *J. Guid., Control, Dyn.*, vol. 40, no. 5, pp. 1304–1313, May 2017.

[9] Q. Shen, C. Yue, C. H. Goh, and D. Wang, "Active fault-tolerant control system design for spacecraft attitude maneuvers with actuator saturation and faults," *IEEE Trans. Ind. Electron.*, vol. 66, no. 5, pp. 3763–3772, May 2019.

[10] A. Noumi and M. Takahashi, "Fault-tolerant attitude control systems for satellite equipped with control moment gyros," in *Proc. AIAA Guid., Navigat., Control Conf.*, 2013, pp. 1–12, AIAA Paper 2013-5119.

[11] J. D. Boskovic and R. K. Mehra, "A decentralized fault-tolerant control system for accommodation of failures in higher-order flight control actuators," *IEEE Trans. Control Syst. Technol.*, vol. 18, no. 5, pp. 1103–1115, Sep. 2010.

[12] B. Wie, D. Bailey, and C. Heiberg, "Rapid multitarget acquisition and pointing control of agile spacecraft," *J. Guid., Control, Dyn.*, vol. 25, no. 1, pp. 96–104, Jan. 2002.

[13] B. Wie, "Singularity escape/avoidance steering logic for control moment gyro systems," *J. Guid., Control, Dyn.*, vol. 28, no. 5, pp. 948–956, Sep. 2005.

[14] C. Yue, Q. Shen, X. Cao, F. Wang, C. H. Goh, and T. H. Lee, "Development of a general momentum exchange devices fault model for spacecraft fault-tolerant control system design," 2019, *arXiv:1907.06751*. [Online]. Available: https://arxiv.org/abs/1907.06751

[15] H. A. Toliyat, S. Nandi, S. Choi, and H. Meshgin-Kelk, *Electric Machines: Modeling, Condition Monitoring, and Fault Diagnosis*. Boca Raton, FL, USA: CRC Press, 2013.

[16] D. Kastha and B. K. Bose, "Investigation of fault modes of voltage-fed inverter system for induction motor drive," *IEEE Trans. Ind. Appl.*, vol. 30, no. 4, pp. 1028–1038, Jul./Aug. 1994.

[17] S. Nandi, H. A. Toliyat, and X. Li, "Condition monitoring and fault diagnosis of electrical motors–A review," *IEEE Trans. Energy Convers.*, vol. 20, no. 4, pp. 719–729, Dec. 2005.

[18] D. Campos-Delgado, D. Espinoza-Trejo, and E. Palacios, "Fault-tolerant control in variable speed drives: A survey," *IET Electr. Power Appl.*, vol. 2, no. 2, pp. 121–134, Mar. 2008.

[19] J. Chen and R. J. Patton, *Robust Model-Based Fault Diagnosis for Dynamic Systems*, vol. 3. New York, NY, USA: Springer, 2012.

[20] J.-W. Zhu, G.-H. Yang, H. Wang, and F. Wang, "Fault estimation for a class of nonlinear systems based on intermediate estimator," *IEEE Trans. Autom. Control*, vol. 61, no. 9, pp. 2518–2524, Sep. 2016.

[21] J. T. Y. Wen and K. Kreutz-Delgado, "The attitude control problem," *IEEE Trans. Autom. Control*, vol. 36, no. 10, pp. 1148–1162, Oct. 1991.

[22] B. T. Costic, D. M. Dawson, M. S. De Queiroz, and V. Kapila, "Quaternion-based adaptive attitude tracking controller without velocity measurements," *J. Guid., Control, Dyn.*, vol. 24, no. 6, pp. 1214–1222, Nov. 2001.

[23] Q. Shen, D. Wang, S. Zhu, and E. K. Poh, "Robust control allocation for spacecraft attitude tracking under actuator faults," *IEEE Trans. Control Syst. Technol.*, vol. 25, no. 3, pp. 1068–1075, May 2017.

[24] W. Luo, Y.-C. Chu, and K.-V. Ling, "Inverse optimal adaptive control for attitude tracking of spacecraft," *IEEE Trans. Autom. Control*, vol. 50, no. 11, pp. 1639–1654, Nov. 2005.

[25] Y. Chen and J. Wang, "Fast and global optimal energy-efficient control allocation with applications to over-actuated electric ground vehicles," *IEEE Trans. Control Syst. Technol.*, vol. 20, no. 5, pp. 1202–1211, Sep. 2012.

[26] J. Nocedal and S. Wright, *Numerical Optimization*. Berlin, Germany: Springer-Verlag, 2006.

[27] W. Chen and M. Saif, "Observer-based fault diagnosis of satellite systems subject to time-varying thruster faults," *J. Dyn. Syst., Meas., Control*, vol. 129, no. 3, pp. 352–356, May 2007.

[28] A. Chunodkar and M. Akella, "Switching angular velocity observer for rigid-body attitude stabilization and tracking control," *J. Guid., Control, Dyn.*, vol. 37, no. 3, pp. 869–878, May-Jun. 2014.

[29] A. W. D. I. Thomas and S. Hebertt, "Variable-structure control of spacecraft attitude maneuvers," *J. Guid., Control, Dyn.*, vol. 11, no. 3, pp. 262–270, 1988.

[30] F. A. Leve and N. G. Fitz-Coy, "Hybrid steering logic for single-gimbal control moment gyroscopes," *J. Guid., Control, Dyn.*, vol. 33, no. 4, pp. 1202–1212, Jul. 2010.